ACKNOWLEDGMENTS

Two of the authors (Y. N. L. and M. D.) wish to thank O. C. Simpson for his interest and encouragement throughout the work. One of the authors (Y. N. L.) expresses thanks to the Associated Midwest Universities for the support he received during the tenure of a Thesis Appointment in the Solid State Science Division of Argonne National Laboratory. The authors thank Duane Larson and Choochon Lee for their invaluable assistance throughout the experiment. It is also a pleasure to acknowledge the patient and helpful work of W. A. Schooley, Mike Mason, and Brad Clymer, the members of the Van de Graff accelerator crew of the Material Research Laboratory at the University of Illinois.

PHYSICAL REVIEW VOLUME 165, NUMBER 3 15 JANUARY 1968

Magnetic Breakdown and Oscillatory Magnetoresistance by a Kubo Formula

W. G. CHAMBERS

Mathematics Department, Westfield College, London, N. W. 3, England

(Received 10 May 1967; revised manuscript received 11 August 1967)

Pippard's effective-path method for calculating the conductivity in a breakdown network is extended by the use of a Kubo formula. It is shown how to calculate oscillations of the conductivity with frequencies in H^{-1} corresponding to (a) the lens orbits in the hexagonal network for Mg and Zn, and (b) the area of the Brillouin zone of the hexagonal network. At fields much greater than the breakdown field, the lens oscillations in the two-dimensional system have the same amplitude as the average conductivity. A rough calculation suggests that in magnesium the lens oscillations should have a magnitude comparable with the triangle oscillations at high fields. The calculations made for the "zone" oscillations are very crude, but it seems quite likely that they are observable.

1. INTRODUCTION

THE discovery of magnetic breakdown[1] has required some modifications in the usual theories of the de Haas–van Alphen effect and of the magnetoresistance. Pippard[2,3] has discussed the consequences of breakdown in terms of network models and the author has attempted to justify this approach in terms of a nearly-free-electron model[4] and in terms of the theory of the effective Hamiltonian.[5] A modified theory of the de Haas–van Alphen effect was developed by Falicov and Stachowiac[6] in terms of a time-dependent Green's function and a similar theory was later developed by the author in terms of a time-independent Green's function.[4,5] Both approaches treat the Green's function as a propagator on a Pippard network.

Falicov and Sievert[7] developed a theory for the magnetoresistance using a Pippard network and the method of Chamber's path integral. Another method was developed by Pippard,[8] which is very simple and powerful when the relaxation caused by impurities and phonons can be neglected. This is called the "effective-path" method. This technique was applied by Falicov, Pippard and Sievert[9] to explain the remarkable oscillations observed by Stark[10] in magnesium and zinc when the magnetic field was aligned along the hexad axis. It has also been applied by Young to explain oscillations in the magnetoresistance observed in tin.[11]

In the case of magnesium and zinc the relevant Pippard network is a hexagonal system of coupled orbits as shown in Fig. 1. The triangles (at K) are very small, and they appear to be responsible for the oscillations. Phase coherence within these triangles was fully taken into account, but it was assumed that phase coherence on the longer arms could be neglected. In consequence the triangles acted as three-way scatterers which came into resonance whenever the magnetic field was such that a Landau level for the triangular orbit was at the Fermi energy. But further experiments by Stark[12] have also detected oscillations caused by the lens orbits, and to explain this it would appear to be necessary to develop a theory which can take phase coherence into account to a higher degree.

The purpose of this paper is to develop such a theory. It is based on the Pippard effective-path method, but this method is extended by the use of a Kubo formula for the conductivity. In order to apply this theory

[1] M. H. Cohen and L. M. Falicov, Phys. Rev. Letters **7**, 231 (1961).
[2] A. B. Pippard, Proc. Roy. Soc. (London) **A270**, 1 (1962).
[3] A. B. Pippard, Phil. Trans. Roy. Soc. (London) **A256**, 317 (1964).
[4] W. G. Chambers, Phys. Rev. **140**, A135 (1965).
[5] W. G. Chambers, Phys. Rev. **149**, 493 (1966).
[6] L. M. Falicov and H. Stachowiac, Phys. Rev. **147**, 505 (1966).
[7] L. M. Falicov and P. R. Sievert, Phys. Rev. **138**, A88 (1965).
[8] A. B. Pippard, Proc. Roy. Soc. (London) **A287**, 165 (1965).
[9] L. M. Falicov, A. B. Pippard, and P. R. Sievert, Phys. Rev. **151**, 498 (1966).
[10] R. W. Stark (to be published).
[11] R. C. Young, Phys. Rev. **152**, 659 (1966).
[12] R. W. Stark (to be published).

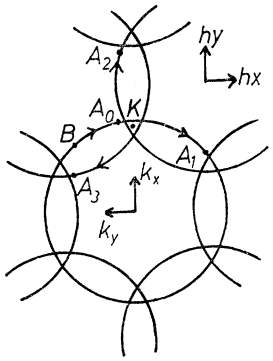

FIG. 1. The hexagonal network for breakdown in the basal plane of the Brillouin zone of magnesium and zinc.

certain propagators have to be evaluated. These propagators are treated by a diagrammatic method similar to that used for the de Haas–van Alphen effect,[6,5] and as much phase coherence as required can be included by summing enough diagrams. This theory thus employs a combination of three methods, the Pippard effective-path method, the theory of propagators on a Pippard network, and a Kubo formula rather than a Boltzmann equation. The development is guided by the theory of the effective path. The treatment of the Kubo formula is not rigorous but it gives an unambiguous answer and the resemblance to the successful theory of Falicov, Pippard, and Sievert should be strong enough to suggest that it is on the right lines.

The theory has been used to calculate two types of oscillations, the lens oscillations, and oscillations which might be called "zone" oscillations, since they correspond to an area equal to the Brillouin zone. No attempt has been made to carry through the calculations to the end but the results suggest that both types of oscillations should be observable. The interest in the "zone" oscillations comes from the theory of the magnetic band structure particularly in two-dimensional models.[3,4] It turns out that the magnetic band structure is very simple when the applied field is such that the area covered by one flux quantum is an integral multiple of the area of the unit cell, but for intermediate values of the field the structure becomes very complicated. This consideration suggests that the properties of the system like the magnetic susceptibility and the resistance should have an oscillation with the "zone" frequency in H^{-1}. However, the theory of the de Haas–van Alphen effect rules this possibility out because there are no orbits with this area, but the theory of the magnetoresistance (though it is not directly concerned with the band structure) suggests that such oscillations should be observable.

The paper is divided up as follows. The next section is a description of the effective path theory as used in the hexagonal network. Section 3 is a treatment of the Kubo formula using propagators on a network. Section 4 describes a self-consistent method for obtaining the effective path and Sec. 5 shows how the theory can be applied to calculating the lens oscillations and the "zone" oscillations. The final section is a brief discussion of the results.

2. THE NETWORK AND THE EFFECTIVE-PATH METHOD

Before commencing the main argument it is convenient to give a description of the Pippard effective-path method[8] and its application to the network models used for magnetic breakdown, because many features of this approach will be adopted with the necessary modifications.

The method is as follows. Suppose we have a specimen of metal to which an electric field $\mathbf{E}$ is applied. We may picture this as causing the Fermi surface to move through $\mathbf{k}$ space. A surface element $d\mathbf{S}$ of the Fermi surface will sweep out a volume of $\mathbf{k}$ space at a rate $e\mathbf{E}\cdot d\mathbf{S}/\hbar$ per unit time, where e is the electronic charge and $\hbar$ is Planck's constant divided by 2π. We may imagine the sweeping process as "creating" particles at a rate $2e\mathbf{E}\cdot d\mathbf{S}/\hbar(2\pi)^3$. (The specimen is taken as having unit volume, and the factor 2 arises from the spin degeneracy.) If we then suppose that these particles travel an average distance $\mathbf{L}(\mathbf{k})$ after "creation" at $\mathbf{k}$, it can be shown that the current $\mathbf{J}$ is given by

$$\mathbf{J}=\frac{2e^2}{8\pi^3\hbar}\int \mathbf{L}\mathbf{E}\cdot d\mathbf{S}=\frac{2e^2}{8\pi^3\hbar}\int \mathbf{L}\mathbf{E}\cdot\mathbf{v}\frac{dS}{v},$$

where $\mathbf{v}$ is the Fermi velocity which is of course directed normal to the Fermi Surface. $\mathbf{L}(\mathbf{k})$ is called the effective path.

We shall only be concerned with two-dimensional models. In this case dS is replaced by the element of arc ds_k on the Fermi curve (which however we shall still call the "surface" by force of habit), and the factor $8\pi^3$ is replaced by $4\pi^2$. The conductivity tensor may then be written as

$$\sigma=\frac{2e^2}{4\pi^2}\int \mathbf{L}\mathbf{v}\frac{ds_k}{v}. \tag{1}$$

We now consider the application of this approach to the hexagonal network used for calculating the magnetoconductivity in magnesium and zinc. The network is the set of coupled orbits which can arise in a two-dimensional hexagonal metal with the magnetic field $\mathbf{H}$ applied along the normal (which is taken to be the z axis). In this case it will be assumed that the Fermi surface is a circle with a diameter just greater that the maximum dimension of the Brillouin zone. The structure in $\mathbf{k}$ space is shown in Fig. 1. In a magnetic field a particle of wave number $\mathbf{k}$ moves along the Fermi surface, and we shall assume that it travels clockwise as indicated by the arrows in Fig. 1. When the particle reaches a junction (a point of Bragg reflection) it may be scattered on to another circle. On any circle

the motion is given by $d\mathbf{k}/dt=\mathbf{v}\times\mathbf{h}$, where

$$\mathbf{h}=e\mathbf{H}/\hbar c \tag{2}$$

(where c is the velocity of light), and the integral of this equation is then

$$\mathbf{k}=\mathbf{r}\times\mathbf{h}+\mathbf{\Pi}, \tag{3}$$

where $\mathbf{\Pi}$ is a constant of integration and $\mathbf{r}$ is the position of the particle in real space. Thus the motion in real space follows a network similar to the $\mathbf{k}$ space network but rotated by 90° and scaled by a factor h^{-1}. The axes on the right of Fig. 1 are used to illustrate this.

The method of calculating the effective path is as follows. The points A_0, A_1, A_2, and A_3 in Fig. 1 will be taken as being just before the nearby junctions. The origin of coordinates will be taken at A_0 and the positions of A_1, A_2, and A_3 will be called $\mathbf{R}_1$, $\mathbf{R}_2$, and $\mathbf{R}_3$, respectively. The effective paths from the points A_i will be called $\mathbf{L}_i$. Suppose now a particle is created at B, whose position vector will be called $-\mathbf{b}$. This particle must migrate to A_0 and its averaged final position must therefore be $\mathbf{L}_0$. Thus the effective path from B is given by

$$\mathbf{L}(B)=\mathbf{b}+\mathbf{L}_0. \tag{4}$$

$\mathbf{L}_0$ is determined as follows. For the sake of simplicity it will be assumed that the triangles are vanishingly small, and that they act as three-way scattering junctions. The probabilities for the scattering of particles coming in from A_0 towards A_1, A_2, and A_3 will be called c_1, c_2, and c_3, respectively. For the sake of conservation these quantities must satisfy

$$c_1+c_2+c_3=1. \tag{5}$$

Then of a number of particles "created" at A_0 a fraction c_1 will travel to A_1 and must finish up on the average at a position $(\mathbf{R}_1+\mathbf{L}_1)$ and similar results will apply for particles scattered towards A_2 and A_3. Thus it will follow that by self-consistency

$$\mathbf{L}_0=c_1(\mathbf{R}_1+\mathbf{L}_1)+c_2(\mathbf{R}_2+\mathbf{L}_2)+c_3(\mathbf{R}_3+\mathbf{L}_3). \tag{6}$$

By the rotational and translational symmetry of the network it must follow that $\mathbf{L}_1=\Omega^{-1}\mathbf{L}_0$, where Ω is the matrix that rotates a vector anticlockwise by 60°. Similarly it must follow that $\mathbf{L}_2=\Omega\mathbf{L}_0$ and $\mathbf{L}_3=\Omega^3\mathbf{L}_0$. Then the following equation determines $\mathbf{L}_0$:

$$(1-c_1\Omega^{-1}-c_2\Omega-c_3\Omega^3)\mathbf{L}_0=c_1\mathbf{R}_1+c_2\mathbf{R}_2+c_3\mathbf{R}_3. \tag{7}$$

Thus the terms $\mathbf{R}_i$ in (6) are the inhomogeneous terms in the equation from which $\mathbf{L}_0$ must be determined.

The actual calculation of the conductivity is straightforward.[9] The features in this argument which we shall attempt to reproduce from a more fundamental viewpoint are (a) the use of a network; (b) an expression like (1) for the conductivity; (c) an effective path satisfying a relation like (4); (d) a self-consistent scheme like (6); and (e) a conservation rule like (5).

3. THE USE OF A KUBO FORMULA

We commence by modifying a Kubo formula for the conductivity so that it is written in a time-independent manner. Then a diagrammatic scheme is set up to represent the propagators in such a formula by means of paths on a Pippard network.

The basic Kubo formula will be taken as[13,14]

$$\sigma_{\mu\nu}=-\lim_{s\to 0+}\operatorname{Re}\operatorname{Tr}[f'(H)J_\mu(s)j_\nu]. \tag{8}$$

Here H is the single-particle Hamiltonian, j_μ is the single-particle current, and $f'(E)$ is the derivative of the Fermi-Dirac distribution function. $J_\mu(s)$ is given by

$$J_\mu(s)=\int_0^\infty e^{-st}e^{iHt}j_\mu e^{-iHt}dt. \tag{9}$$

We shall set $j_\mu=ev_\mu$, where $\mathbf{v}$ is the velocity.

$f'(H)$ is represented as

$$f'(H)=\int_{-\infty}^{\infty}f'(E)\delta(E-H)dE, \tag{10}$$

and then we need to evaluate

$$X_{\mu\nu}=e^2\operatorname{Tr}\left\{\int_0^\infty\delta(E-H)e^{-st}e^{iHt}v_\mu e^{-iHt}v_\nu dt\right\} \tag{11}$$

in the limit $s\to 0+$. By the property of the δ function we can replace H by E in an adjacent factor, and then the integration is simple. It gives

$$X_{\mu\nu}=e^2\operatorname{Tr}\{\delta(E-H)v_\mu(s-iE+iH)^{-1}v_\nu\}.$$

We introduce the coordinate operator by

$$v_\mu=i(Hx_\mu-x_\mu H),$$

and we define the propagators or Green operators by

$$G_{\pm s}=(E\pm is-H)^{-1}. \tag{12}$$

By the use of the formulas $\delta(E-H)H=\delta(E-H)E$ and $is\delta(E-H)G_{+s}=\delta(E-H)$, we can obtain

$$X_{\mu\nu}=e^2\operatorname{Tr}\{\delta(E-H)is(x_\mu G_{+s}-G_{+s}x_\mu)v_\nu\}. \tag{13}$$

We also need the formula

$$2\pi i\delta(E-H)=G_{-0}-G_{+0}, \tag{14}$$

where $G_{\pm 0}=\lim_{s\to 0+}G_{\pm s}$.

It is now necessary to show how the propagators can be treated by a diagrammatic method.[5] We shall use the simplest possible scheme, a nearly-free-electron system[4] with a periodic potential dependent on one

[13] This formula is like the one suggested by G. V. Chester and A. Thellung [Proc. Phys. Soc. (London) **73**, 745 (1959)] but the cutoff in the time integration is represented by an exponential cutoff [I. Mannari, Progr. Theoret. Phys. (Kyoto) **26**, 51 (1961)] and according to E. Verboven [Physica **26**, 1091 (1960)] only the real part is used.

[14] See, for instance, J. M. Ziman, *Principles of the Theory of Solids* (Cambridge University Press, New York, 1964), p. 279.

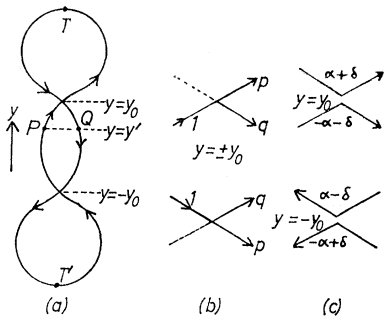

FIG. 2. (a) Linear network for one-dimensional model. (b) Scattering amplitudes. (c) "Extrinsic" phase shifts for Bragg reflection.

dimension only. The units will be chosen so that $h=2m=1$, where m is the electronic mass. The kinetic momentum $\mathbf{P}$ is equal to $\mathbf{p}-\mathbf{A}$, where $\mathbf{p}$ is represented by $-i\nabla$ and curl $\mathbf{A}=\mathbf{h}$, where $\mathbf{h}$ is given by (2). We also need the operator

$$\mathbf{\Pi}=\mathbf{P}+\mathbf{h}\times\mathbf{x}, \tag{15}$$

which is the quantum analog of the quantity $\mathbf{\Pi}$ in (3). $\mathbf{\Pi}$ commutes with $\mathbf{P}$ (and therefore also with the kinetic energy $\mathbf{P}^2$) and its components satisfy the commutation rule

$$\Pi_x\Pi_y-\Pi_y\Pi_x=-ih. \tag{16}$$

The Hamiltonian will be taken as

$$H=P_x^2+P_y^2+2V_0\cos(2\pi y/b). \tag{17}$$

Here V_0 is the strength of the periodic potential and b is the lattice spacing. With a Landau gauge $\mathbf{A}=(-hy, 0, 0)$ the Schrödinger equation $H\psi=E\psi$ can be satisfied by

$$\psi(x,y)=e^{iq_xx}u(y+q_x/h), \tag{18}$$

where $u(y)$ is a solution of

$$\{-d^2/dy^2+h^2y^2-E+2V_0\cos[2\pi(y/b)-\alpha]\}\times u(y)=0, \tag{19}$$

where

$$\alpha=2\pi q_x/bh. \tag{20}$$

$\psi(x,y)$ is an eigenfunction of Π_x with eigenvalue q_x, and the origin of y has been shifted in (18) for convenience.

The free-electron travelling wave solutions for (19) (with $V_0=0$) are in the Wentzel-Kramers-Brillouin (WKB) approximation

$$u_\pm(y)=[v(y)]^{-\frac{1}{2}}e^{\pm iJ(y)}, \tag{21}$$

where

$$J(y)=\int^y k(\eta)d\eta. \tag{22}$$

Here $k(y)=(E-h^2y^2)^{1/2}$ is the y component of the momentum and $v(y)=2k(y)$ is the y component of the velocity. Bragg reflection occurs at the points $y=\pm y_0$, where $k(y_0)=\pi/b$, and it will be assumed that E and b are such that there are only two such points.

The propagation of the solutions can be described on a one-dimensional network as shown in Fig. 2(a).[4] The solution u_+ is pictured as propagating upwards. When it reaches the turning point T it is reflected and returns as u_-. But when V_0 is not equal to zero, there is also Bragg reflection at $y=\pm y_0$. At these points we shall call the transmission amplitude p and the reflection amplitude q [Fig. 2(b)]. For unitarity we must have $p^*p+q^*q=1$, $p^*q+q^*p=0$. There are also "extrinsic" phase shifts upon Bragg reflection, determined by the phase of the position of the reflection points $\pm y_0$ with respect to the periodic potential.[4] These are given in Fig. 2(c). Here δ is equal to $2\pi y_0/b$ and α is given by (20). The method of determining the eigenvalues in such a network has been considered elsewhere.[2,4]

The Green's function $G_{+0}(y,y')$ is the solution of an equation like (19) but with a term $-\delta(y-y')$ on the right-hand side. y' can be regarded as a source point radiating outgoing waves and so the Green's function contains the term

$$-iu_+(y_>)u_-(y_<), \tag{23}$$

where $y_>$ and $y_<$ are the greater and lesser, respectively, of y and y'. The other terms in the Green's function can be regarded as being caused by the reflections. Each term can be represented as a path in Fig. 2(a) following the arrows. A wave starting upwards (or downwards) at $y=y'$ is pictured as commencing at P (or Q).

However it is in many ways better to represent the path on a Pippard network[2] in real space, as shown in Fig. 3. We shall use the following notation. Positions on the network will be denoted by $\mathbf{r}$, $\mathbf{r}'$, etc., and the position along the y axis by y, y', etc. The y component of the velocity will be written as $v(y)$, and the actual velocity at the point $\mathbf{r}$ as $\mathbf{v}(\mathbf{r})$, and its magnitude as $v(\mathbf{r})$. The network does not have to represent anything "actual," though it is possible to set up wave functions lying on the network.[5] The main difference from the network of Fig. 2(a) is that every time a wave is Bragg-reflected upwards (downwards) it is transferred one circle to the right (left).

For the sake of illustration let us consider the contribution to $G_{+0}(y_2,y_1)$ represented by the path in Fig. 3 from $\mathbf{r}_1$ to $\mathbf{r}_2$ drawn as a heavy line. This contribution is

$$g(\mathbf{r}_2,\mathbf{r}_1)=-ic[v(y_1)v(y_2)]^{-\frac{1}{2}}e^{i\varphi}, \tag{24}$$

where the coefficient c is the product of the scattering amplitudes, pq in this case, and φ is the sum of the extrinsic phase $(\alpha+\delta)$ and the propagation phase which is given by the upper shaded area times h. δ is also represented by an area in this diagram. Then we sum over both values of $\mathbf{r}_1$ (with y coordinate y_1) on one arbitrarily chosen circle (called the "primary" circle)

and over all possible values of $\mathbf{r}_2$ (with y coordinate y_2) on the network, and over all possible paths following the arrows and joining $\mathbf{r}_1$ and $\mathbf{r}_2$. There is one exception to this rule. When $y_1=y_2$, it is possible to have $\mathbf{r}_1=\mathbf{r}_2$ at two points, with two corresponding "paths" of zero length joining them. But only one of these must be counted, and the contribution to $G_{+0}(y,y)$ is just $-i[v(y)]^{-1}$ from (23).

As an example and for later use we now consider the evaluation of the energy density of states[5,6]

$$n(E)=\mathrm{Tr}\delta(E-H).$$

By (14) this can be written as

$$n(E)=-(2\pi)^{-1}\,\mathrm{Tr}\{i(G_{-0}-G_{+0})\}. \tag{25}$$

Suppose the metal has dimensions A in the x direction and B in the y direction. Taking the trace involves integrating over y and over q_x. It is sufficient to integrate over y between the turning points, and the range of integration over q_x can be taken from 0 to hB, since such a shift in q_x moves the center of the line of orbits by a distance B in the y direction. Thus we have to evaluate

$$-\frac{A}{(2\pi)^2}\int dy\int_0^{Bh} dq_x 2\,\mathrm{Im}G_{+0}(y,y). \tag{26}$$

G_{+0} is of course a function of q_x. The important point is that the only terms in G which contribute are represented by closed orbits. We can give the following reason.[5] If a path commencing upwards (at P, say) finishes downwards (at Q, say) then the propagation phase shift varies rapidly with y and the contribution goes out by "random phase." Thus we need only include paths which return in the same direction as they set out. But if a path finishes on a different circle, then its phase contains a multiple of α from the "extrinsic" phase shifts and so when the integration over q_x (on which α depends) is performed this contribution must also go out. So in the end we are left with closed paths. The sum of the propagation phase shifts and the "extrinsic" phase shifts is simply the area of the orbit times h. Such a term is of course independent of q_x.

Another reason can be given why only closed orbits can contribute. The propagation phases are measured by areas, but for open paths the area is not unique and depends on the gauge. Thus we can argue that gauge invariance requires that the orbits be closed.

We now reconsider (26). The terms that are kept are independent of q_x. They also contain a factor $[v(y)]^{-1}$ besides the phase factors and the attenuation factors. It is then possible to write $dr/v(\mathbf{r})$ instead of $dy/v(y)$, where dr is an element of arc on the network. The final result is then

$$n(E)=\frac{AB}{(2\pi)^2}\int\frac{hdr}{v(\mathbf{r})}\Delta(\mathbf{r}), \tag{27}$$

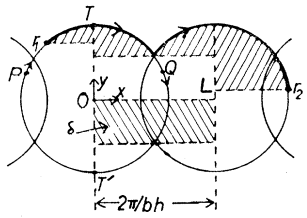

FIG. 3. Pippard network for one-dimensional model. Areas giving certain phase shifts are shaded.

where

$$\Delta(\mathbf{r})=1+2\,\mathrm{Re}\sum_p c_p(\mathbf{r})e^{i\varphi_p(\mathbf{r})}. \tag{28}$$

In this formula the sum is taken over all closed paths following the arrows from $\mathbf{r}$ back to $\mathbf{r}$. $c_p(\mathbf{r})$ is the product of all the scattering amplitudes on the path p. The phase factor $\varphi_p(\mathbf{r})$ is given by h times the area of the orbit p in real space, or alternatively by h^{-1} times the area of the equivalent orbit in $\mathbf{k}$ space. The integration in (27) is confined to the "primary" circle in the network. The first term on the right-hand side of (28) comes from the path of "zero length" as described above.

In a similar way (13) can be expressed as a sum of terms represented by diagrams. We replace the δ operator by (14), and there are two contributions to X. The one which will prove to be important is

$$X_{\mu\nu}^{(1)}=e^2(2\pi)^{-1}\ \mathrm{Tr}\{sG_{-0}(x_\mu G_{+s}-G_{+s}x_\mu)v_\nu\}, \tag{29a}$$

and the other is

$$X_{\mu\nu}^{(2)}=e^2(2\pi)^{-1}\ \mathrm{Tr}\{-sG_{+0}(x_\mu G_{+s}-G_{+s}x_\mu)v_\nu\}. \tag{29b}$$

In the scheme described above the operators x_μ and $P_\nu=\frac{1}{2}v_\nu$ are represented as follows:

$$\begin{aligned} x_2&=y, \quad P_2=-i\partial/\partial y,\\ P_1&=hy, \quad x_1=h^{-1}(-i\partial/\partial y-ih\partial/\partial q_x). \end{aligned} \tag{30}$$

P_1 would be q_x+hy were it not for the shift in the y coordinate in (18). The representation of x_1 is obtained from (15) and (16). The propagator G_{+s} is much the same as G_{+0}, but there is also an attenuation factor. The operator G_{-0} is the Hermitian conjugate of G_{+0}, and it will be represented by paths traveling against the arrows of the network. Its representation satisfies $G_{-0}(y,y')=[G_{+0}(y',y)]^*$. A differential operator on the extreme right of the trace operates on the extreme left.

The derivative operators $-i\partial/\partial y$ in (30) acting on a term of a Green's function like (24) simply give the momentum k_y as measured on the "primary" circle of the $\mathbf{k}$ space network. Thus in particular $-ih^{-1}\partial/\partial y_2 \times g(\mathbf{r}_2,\mathbf{r}_1)$ will give the length $L\mathbf{r}_2$ in Fig. 3. The operator $-i\partial/\partial q_x$ measures the number of times α appears in the "extrinsic" phase and hence how many circles the path has gone to left or right in Fig. 3. All in all we find that $\mathbf{x}$ and $\mathbf{v}$ acting on a term $g_{\pm0}(\mathbf{r}_2,\mathbf{r}_1)$ of $G_{\pm0}(y_2,y_1)$ give $\mathbf{r}_2$ and $\mathbf{v}(\mathbf{r}_2)$ times the term.

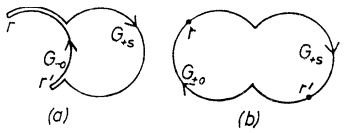

FIG. 4. Diagrams for the effective path.

This result assumes that we may neglect the derivatives of $[v(y)]^{-\frac{1}{2}}$ which appear in the Green's function and the commutators of $\mathbf{x}$ and $\mathbf{v}$. Such terms are presumably one order higher in h than the terms just considered, or alternatively are reduced by a factor (h/E_F) where E_F is the Fermi energy. Moreover they are imaginary and will not contribute to (8).

We now express (29a) as a sum of terms which are represented by closed diagrams on a Pippard network. We may as before argue that the diagrams are closed for reasons of gauge invariance, or that the terms left out vary rapidly with y or q_x and so must go out when the integrations are performed. The formula for $X^{(1)}$ may then be written as

$$X^{(1)}=e^2\frac{AB}{(2\pi)^2}\int\frac{hdr}{v(\mathbf{r})}\mathbf{L}(\mathbf{r})\mathbf{v}(\mathbf{r}), \tag{31}$$

where

$$\mathbf{L}(\mathbf{r})=v(y)\frac{s}{2\pi}\int_{r'}G_{-0}(\mathbf{r},\mathbf{r}')(\mathbf{r}'-\mathbf{r})G_{+s}(\mathbf{r}',\mathbf{r}). \tag{32}$$

With AB set equal to unity, (31) is equivalent to (1). Here $G(\mathbf{r},\mathbf{r}')$ is the sum of the subset of terms of $G(y,y')$ which are represented by all paths going from $\mathbf{r}'$ to $\mathbf{r}$ on the network. We restrict $\mathbf{r}$ to the two points on the "primary" circle with y coordinate y, but $\mathbf{r}'$ can be any of the points with y coordinate y'. To obtain $G(y,y')$ we have to sum over all these possible values of $\mathbf{r}$ and $\mathbf{r}'$. Thus we represent the integration over y by the integral over $\mathbf{r}$ in (31) restricted to the "primary" circle. But the integration over y' is represented by an integration over $\mathbf{r}'$ all over the network, and in this way the summation over the values of $\mathbf{r}$ and $\mathbf{r}'$ is automatically taken into account. Moreover we need keep only those terms in the product $G_{-0}G_{+s}$ which are represented by closed diagrams because the others go out by "random phase" in the integrations over y in (31) and over q_x (implicit in the trace operation). G_{+s} propagates with the arrows of the network and G_{-0} against them. The sum of the propagation phases and the extrinsic phases is given by the area of the diagram times h. Areas encircled clockwise (anticlockwise) are considered positive (negative). We also multiply together the scattering amplitudes at the junctions, but we use the complex conjugates when the junctions are on the return path.

We may now consider the term (29b). A similar diagrammatic expansion is possible, but this time both paths must go with the arrows. [A typical diagram is shown in Fig. 4(b).] In the limit $s\rightarrow 0+$ we shall assume that the term vanishes for the following reason. There are only a finite number of diagrams with a perimeter less than some given length. In the limit $s\rightarrow 0+$ the contribution of these diagrams goes to zero because of the factor s in (29). Thus the contributions can only come from diagrams of very large perimeter. Since the return path cannot go back along the outgoing path such diagrams will have large areas on the whole and presumably the sum will vanish by "random phase." The argument is stronger if the effect of thermal averaging at a finite temperature is considered. Orbits of very large perimeter have a very low cyclotron frequency and their contributions will be "washed out" just as in the theory of the de Haas–van Alphen effect. If for any reason it seems possible that these terms can contribute to the conductivity then their sum can be added in later, but it seems very unlikely that this is so.

We return to considering the terms in (29). In this instance we have a class of diagrams (to be called "zero-area" diagrams) where the return propagator comes back along the outgoing path. These diagrams must give a contribution which is not oscillatory in h^{-1}, and they are presumably the ones which can be treated by the standard effective-path method. Similarly there will be a class of diagrams where the return path differs from the outgoing path only by the inclusion of a single loop of a given area. These terms will all be phase-coherent, even though the lengths of the paths may be very large. Since no one diagram contributes finitely in the limit $s\rightarrow 0+$, a self-consistent method will be used, just like the effective-path method.

The extension to a two-dimensional network should be straightforward. As an illustration we shall use a two-dimensional rectangular lattice with a period a in the x direction.[4,5] We may apply periodic boundary conditions over a distance $B=Nb$, where N is some integer, if the magnetic field h satisfies $h=(2\pi/ab)\times(\lambda/N)$, where λ is some integer. This time, however, Π_x does not commute with the Hamiltonian, and we have to use the magnetic translation operator $\tau=e^{ia\Pi_x}$ instead. With it we may associate eigenvalues e^{iaq_x} where the range of q_x is 0 to $2\pi/a$ instead of 0 to $hB(=2\pi\lambda/a)$ as before. The network now consists of λ links along the y direction instead of the one link as shown in Fig. 4(a). The integration over y takes in all these links and if we keep y on the "primary" link this introduces a factor λ which exactly compensates for the decrease in the range of q_x. Thus in (31) and (32) we again keep $\mathbf{r}$ on the "primary" circle, but $\mathbf{r}'$ can wander all over the two-dimensional network.

4. THE SUMMATION OF THE DIAGRAMS

Let us suppose that we somehow know the effective path $\mathbf{L}(\mathbf{r}_1)$ from some point on a network and we wish to calculate $\mathbf{L}(\mathbf{r}_1-\mathbf{a})$ from a preceding point $(\mathbf{r}_1-\mathbf{a})$ on the same arm of the network. It is evident that

except for one diagram where the final point $\mathbf{r}'$ is between $(\mathbf{r}_1-\mathbf{a})$ and $\mathbf{r}_1$, both the outgoing and return paths from $(\mathbf{r}_1-\mathbf{a})$ must pass through $\mathbf{r}_1$. This exceptional diagram gives no contribution in the limit $s\rightarrow 0+$ and can be ignored. Moreover the product of the propagators and of the term $v(y)$ in (32) is unchanged if we start the diagram at $\mathbf{r}_1$ rather than $(\mathbf{r}_1-\mathbf{a})$. Thus we shall have

$$\mathbf{L}(\mathbf{r}_1-\mathbf{a})=\frac{v(y_1)}{2\pi}\lim_{s\rightarrow 0+} s\int_{r'} G_{-0}(\mathbf{r}_1,\mathbf{r}')(\mathbf{r}'-\mathbf{r}_1+\mathbf{a}) \times G_{+s}(\mathbf{r}',\mathbf{r}_1)$$
$$=\mathbf{L}(\mathbf{r}_1)+\mathbf{a}\Delta(\mathbf{r}_1,\mathbf{r}_1), \tag{33}$$

where

$$\Delta(\mathbf{r},\mathbf{r})=v(y)\lim_{s\rightarrow 0+}\frac{s}{2\pi}\int_{\mathbf{r}'} G_{-0}(\mathbf{r},\mathbf{r}')G_{+s}(\mathbf{r}',\mathbf{r}). \tag{34}$$

This expression looks like a matrix element of the operator product

$$sG_{-0}G_{+s}=i(G_{+s}-G_{+0})+2\pi\delta(E-H), \tag{35}$$

which follows from (12) and (14). In the limit $s\rightarrow 0+$ the first term on the right vanishes. The integration in (34) is the integration over y' of a subset of "gauge-invariant" terms of the product $G_{-0}(y,y')G_{+s}(y',y)$, which are peculiar in that they do not change rapidly with y and in that they are independent of q_x. Thus by (35) and (14) the result must be a subset of terms of $\mathrm{Im}G_{+0}(y,y)$ with the same properties, in fact the terms which appear in the expression for the energy density of states (26). The factor $v(y)$ in (34) cancels out a similar factor in the denominator of the Green's function, and thus we may identify $\Delta(\mathbf{r},\mathbf{r})$ with $\Delta(\mathbf{r})$ given by (28). According to (27) the appropriate integration of $\Delta(\mathbf{r})$ over one circle of the network gives the energy density of states, and $\Delta(\mathbf{r})$ can be regarded as the ratio of the actual density of states at $\mathbf{r}$ (or at the corresponding point in $\mathbf{k}$ space) to the density of states $[v(\mathbf{r})]^{-1}$ in the usual theory.

Thus in the generalized theory (33) has replaced (4). We are now ready to set up the self-consistent theory. Because of (33) it is sufficient to determine the effective path $\mathbf{L}(\mathbf{r})$ from some point just before a junction (like A_0 in Fig. 1). For convenience both propagators will be drawn following the arrows of the network, though of course the arrows on the return path should be reversed.

Figure 5(a) represents some portion of a network. Let us choose A_0 as the origin, and let the positions of the points A_i be $\mathbf{R}_i$. Let the amplitudes for transmission and reflection be p and q. To calculate $\mathbf{L}(A_0)$ we commence the paths at A_0. At the neighboring junction two different possibilities arise. Either the paths remain together until at least the next junction [Figs. 5(b) and 5(c)] or they branch [Fig. 5(d)]. In the former case the diagram is always terminated just before the next

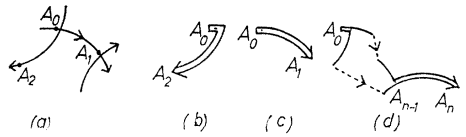

FIG. 5. Terminated diagrams in the self-consistent method.

junction [at A_1 and A_2 in Figs. 5(b) and 5(c)] because it will be assumed that the effective paths $\mathbf{L}(A_1)$ and $\mathbf{L}(A_2)$ are known. If the paths branch we follow them until they coalesce on to the same arm at some junction A_{n-1} [Fig. 5(d)] and then they are terminated just before the very next junction A_n. (If the paths come together at A_{n-1} and then branch again we do not terminate the diagram at this point. We must wait until the paths coalesce on to the same arm of the network.) If as in Fig. 6(c) one of the paths coalesces with the other path that has just begun, then the diagram is terminated not immediately, but at the following junction. Thus a diagram is terminated just before a junction if and only if the paths have coalesced at a junction immediately preceding. It is not suggested that the above scheme is the only way of summing the diagrams, but it seems the most obvious method. The branching diagrams have a complex conjugate where the roles of the two paths are interchanged. Thus the above diagrams will give rise to the equation

$$\mathbf{L}(A_0)=p^*p[\mathbf{L}(A_1)+\mathbf{R}_1\Delta(A_1)]+q^*q[\mathbf{L}(A_2) +\mathbf{R}_2\Delta(A_2)]+\textstyle\sum_n (2\,\mathrm{Re}c_n e^{i\theta_n}) \times[\mathbf{L}(A_n)+\mathbf{R}_n\Delta(A_n)]. \tag{36}$$

The sum is over all possible diagrams of the type in Fig. 5(d). c_n and θ_n are determined as follows. We reverse the path of one of the propagators in Fig. 5(d). The propagation phase shift θ_n is given by the area of the diagram times h. Areas encircled clockwise or anticlockwise are treated as positive or negative, respectively. c_n is given by the product of the scattering amplitudes on the outgoing path and of the complex conjugates of the scattering amplitudes on the return path. Equation (36) is then the generalization of (6).

We can also use this approach for the expression (34) rather than (32). We obtain an equation like (36) but this time $\mathbf{L}(A_0)$ is replaced by $\Delta(A_0)$ and the expressions $[\mathbf{L}(A_i)+\mathbf{R}_i\Delta(A_i)]$ by $\Delta(A_i)$. Such an equation should represent the conservation of particles. When an approximate expression for the effective path is derived by summing only a subset of all possible diagrams, it is important to check that the conservation rule is obeyed. This is actually quite easy to arrange, as will be seen in the examples of the next section.

Presumably this theory will fail to give answers converging to anything sensible in the limit as the number of diagrams summed is increased without limit, since we are calulating the conductivity of what is in effect a perfect lattice. So it is pertinent to inquire whether the theory can be used at all. Pippard has argued that

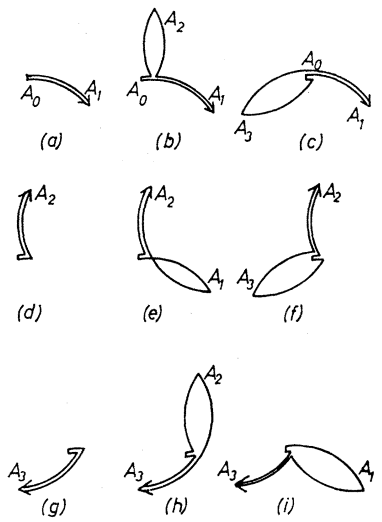

FIG. 6. Diagrams with up to one lens orbit.

in very pure specimens the principal relaxing mechanism is not impurity scattering but phase incoherence in the Bragg reflections which is produced by dislocations.[8] This will presumably affect most the diagrams enclosing large areas and containing many points of Bragg reflection. Thus a judicious selection of only the smaller diagrams for summation should give results that will relate to experimental data. This is evidently only an approximate method of taking the phase incoherence into account, but the answers should be adequate because of the great difficulty of obtaining accurate experimental results.

5. SOME CALCULATIONS

A. Lens-Orbit Oscillation in First Order

The diagrammatic method will be illustrated by a calculation of the oscillations in the conductivity caused by the lens orbits. Only diagrams with one lens orbit will be included for simplicity, and presumably this approximation will be adequate since it is probably rather difficult to observe the harmonics. It will also be assumed for simplicity that the triangles are very small.

The amplitudes for scattering of a wave coming in from A_0 by the triangle centered on K in Fig. 1 will be taken as p, q, r in the directions of A_1, A_2, and A_3, respectively. By the threefold symmetry the scattering matrix is

$$\begin{bmatrix} p & q & r \\ r & p & q \\ q & r & p \end{bmatrix},$$

and the conditions for unitarity are

$$p^*p+q^*q+r^*r=1, \tag{37a}$$

$$p^*q+q^*r+r^*p=0. \tag{37b}$$

These amplitudes can be calculated by the method of Falicov, Pippard and Sievert.[9] If the "intrinsic" scattering amplitudes at a junction are τ for transmission and ρ for reflection, then they must satisfy $\tau^*\tau+\rho^*\rho=1$, $\tau^*\rho+\rho^*\tau=0$. $|\tau|^2$ is given by $\exp(-H_B/H)$, where H is the applied field and H_B the breakdown field. This leaves one free parameter, the phase of τ (or ρ). The phase shift for propagation around the triangle will be called T. To satisfy the unitarity condition (37b) we may introduce this phase as "extrinsic" phase of $\frac{1}{3}T$ for reflections inside the triangle (and a corresponding phase of $-\frac{1}{3}T$ outside) and forget about the propagation phases. Then if we define $\rho_1=\rho e^{iT/3}$, $\rho_2=\rho e^{-iT/3}$, the scattering amplitudes are given by

$$p=\tau^2(1-\rho_1^3)^{-1}, \quad r=\rho_1\tau^2(1-\rho_1^3)^{-1},$$
$$q=\rho_1^2\tau^2(1-\rho_1^3)^{-1}+\rho_2. \tag{38}$$

After this stage the size of the triangles will be neglected, and they will be treated as three-way scattering junctions.

The phase for propagation around the lens orbits will be called L. Then to first order the factor for the energy density of states $\Delta(\mathbf{r})$ is given by

$$\Delta=1+2\ \mathrm{Re}(r^2e^{iL}) \tag{39}$$

and is independent of the position on the network. There are nine diagrams altogether for the effective path $\mathbf{L}(A_0)$, as shown in Fig. 6. We then obtain an equation like (6), but this time $\mathbf{R}_1$, $\mathbf{R}_2$, and $\mathbf{R}_3$ are multiplied by a coefficient Δ, and c_1, c_2, and c_3 are given by

$$c_1=p^*p+2\ \mathrm{Re}[e^{iL}(p^*q^2r+p^*pr^2)],$$
$$c_2=q^*q+2\ \mathrm{Re}[e^{iL}(q^*p^2r+q^*qr^2)], \tag{40}$$
$$c_3=r^*r+2\ \mathrm{Re}[e^{iL}(2r^*pqr)].$$

Since Δ is the same at all points, we may in this case leave it out until the end, when it is used as a factor in the answer. In this way the de Haas–Shubnikov oscillations due to the density of states are introduced. The method of calculation of the conductivity is just the same as that given by Falicov, Pippard, and Sievert.[8,9]

The self-consistent method involves an inversion and so it is apparent that terms proportional to $\cos L$ and $\sin L$ will appear in the denominator of the expression for the conductivity. Therefore the conductivity should be expanded as a power series in such terms and only the first-order terms should be kept. Otherwise we are in effect doing a partial sum of (unterminated) diagrams with two or more lens orbits. It would of course be best if a complete sum over all possible orders could be carried out.

It can readily be shown that the above choice of diagrams obeys the conservation rule. In (6) we replace $\mathbf{L}_0$ and $(\mathbf{R}_i+\mathbf{L}_i)$ by $\Delta(A_0)$ and $\Delta(A_i)$. Since Δ is the same everywhere, this simply means that the coefficients c_i must satisfy (5). It is evident from (40) that since e^{iL} is of arbitrary phase the coefficients of this

quantity must add up to zero. The terms independent of e^{iL} must add up to 1. These results follow from (37).

It seems that in most cases conservation can be arranged almost automatically as follows. In any final coalescence all three possible ways that the paths can go to the terminating junctions must be summed (Fig. 7). The contribution to the propagators from these parts of the diagrams are, respectively, pq^*, rp^*, and qr^* (if the propagator coming in from the left is taken as the outward propagator). It is then evident from (37b) that the sum of the appropriate terms in the conservation equation must be zero.

B. "Zone" Oscillations

As another example we shall discuss some diagrams where the area is that of the primitive cell in the network. Periodicities corresponding to such an area (the area of the Brillouin zone in $\mathbf{k}$ space) are not found in the de Haas–van Alphen effect, because there are no closed orbits following the arrows of the network with this area. Hence we shall set $\Delta=1$, because there is no de Haas–Shubnikov effect with such a period. The area is given by $(C-3L)$, where C is the area of the circle, and L the area of a lens.

There are nine diagrams with the lowest possible number of passages through junctions (eight). Three of these are shown in Figs. 8(a), 8(b), and 8(c), and the others are constructed as indicated in Fig. 7. Thus the conservation rule is obeyed. A diagram with ten junctions is shown in Fig. 8(d), but we shall not consider these higher order diagrams any further. Besides those nine diagrams we also shall use the diagrams of Figs. 6(a), 6(d), and 6(g). The terminal points are marked in Fig. 8(e). The following equation is obtained for the effective path $\mathbf{L}_0$ from 0 (which is the same as A_0 in Fig. 1):

$$\mathbf{L}_0=p^*p[\mathbf{R}_1+\mathbf{L}(A_1)]+q^*q[\mathbf{R}_2+\mathbf{L}(A_2)]+r^*r[\mathbf{R}_3+\mathbf{L}(A_3)]+\sum_{n=1,9}(\mathbf{X}_n+\mathbf{L}_n)g_n,$$

where $\mathbf{R}_1$, $\mathbf{R}_2$, and $\mathbf{R}_3$ are the positions of A_1, A_2, and A_3, the $\mathbf{X}_n$ are as shown in Fig. 8(e), and the coefficients g_n are given by $g_n=2\,\mathrm{Re}(e^{i\theta}\alpha_n)$, where θ is the propagation phase around the orbit, and the α_n are given by

$$\alpha_1=qp^2(qp^*)q^{*2}p^*,\quad \alpha_5=p^3(rq^*)q^{*2}r^*,\quad \alpha_4=rp^2(pr^*)q^{*3},$$
$$\alpha_2=qp^2(rq^*)q^{*2}p^*,\quad \alpha_8=p^3(pr^*)q^{*2}r^*,\quad \alpha_6=rp^2(qp^*)q^{*3},$$
$$\alpha_3=qp^2(pr^*)q^{*2}p^*,\quad \alpha_9=p^3(qp^*)q^{*2}r^*,\quad \alpha_7=rp^2(rq^*)q^{*3}.$$

The $\mathbf{L}_n$ are the effective paths from $\mathbf{X}_n$ and the rotational symmetry relates them to $\mathbf{L}_0$ as follows:

$$\mathbf{L}_1,\ \mathbf{L}_4,\ \mathbf{L}_5=\mathbf{L}_0;\quad \mathbf{L}_2,\ \mathbf{L}_6,\ \mathbf{L}_8=\omega\mathbf{L}_0;\quad \mathbf{L}_3,\ \mathbf{L}_7,\ \mathbf{L}_9=\omega^2\mathbf{L}_0,$$

where ω is the operator that rotates a vector anticlockwise by 120°. In this way a self-consistent equation for $\mathbf{L}_0$ is obtained.

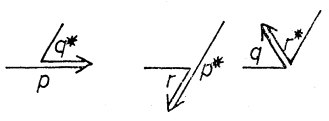

FIG. 7. Three ways of terminating a diagram.

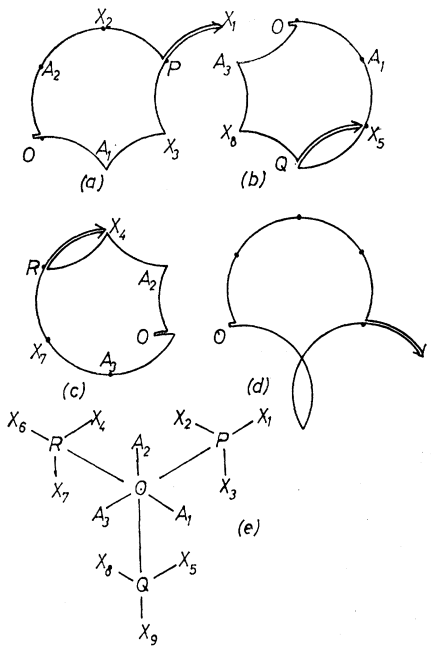

FIG. 8. (a)–(d) Diagrams for the zone oscillations. (e) Positions of the terminating points.

6. SOME RESULTS

Some numerical computations were carried out, but they will not be discussed at great length since with the limited number of diagrams used the results are not likely to be very accurate. However, they should be an adequate guide.

The lens oscillations are discussed first. The most important parameter is the ratio of the applied field H to the breakdown field H_B. At low values of this ratio the lens oscillations certainly show up but not in any especially interesting manner. The magnitude was comparable with that which would be obtained by using only the de Haas–Shubnikov theory, that is, by ascribing the oscillations to the oscillations in the density of states Δ. At high fields ($H\gtrsim 5H_B$) the lens oscillations become rather strong. They dominate the triangle oscillations and have an amplitude roughly equal to the average conductivity. For $H\gtrsim 8H_B$ the diagonal conductivity becomes slightly but definitely negative at the bottom of some cycles. This disconcerting result will be considered in a moment.

We may make an estimate of the ratio of the amplitude of the lens oscillations to that of the triangle oscillations for magnesium as follows. We shall choose

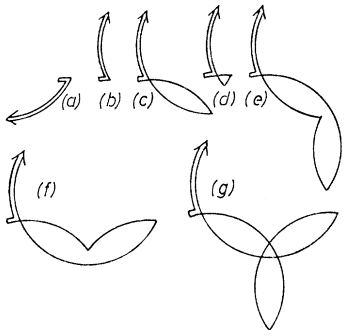

FIG. 9. Diagrams for the lens and triangle oscillations in the high-field region.

$H=35$ kG and the temperature as 1.2°K. We shall take the cyclotron mass m^* for the lens orbit as 0.4 simply because the perimeter is 0.4 times the free-electron circle; this value is obtained if the perimeter of the free-electron triangle is 0.1 times the perimeter of the circle.[9] We shall take the breakdown field at 7 kG. Then numerical calculations give the ratio as about 1.7 in the two-dimensional model. At 1.2°K the thermal damping factor[9] [from the integration in (10)],

$$\zeta=X/\sinh X, \quad \text{with} \quad X=2\pi^2(m^*/m)kT/(ehH/mc),$$

is then about 0.6 for the lens orbit and very nearly 1.0 for the triangle. The integration over k_z gives an extra factor proportional to $(\partial^2 A/\partial k_z^2)^{-\frac{1}{2}}$ where A is the area of the appropriate orbit in **k**-space. The ratio of these factors for the two orbits is given by the inverse square root of the ratio of the effective masses; that is, 0.5. Thus the ratio of the amplitude of the lens oscillations to that of the triangle oscillations is $1.7\times0.6\times0.5$ which is just over 0.5. (If the de Haas–Shubnikov theory alone is used for the lenses the ratio is about 0.25.) This is a very rough figure, particularly since the breakdown field is not well known. As the breakdown field is increased the ratio falls.

We now look at the theory for the conductivity at high fields to see why it may give negative results. In terms of the coefficients c_1, c_2, and c_3 in (6) the conductivity (appropriately scaled) can be written thus:

$$\sigma H=[-\tfrac{1}{2}i\pi+\tfrac{3}{2}K(1+\omega^2K)^{-1}]\Delta, \tag{41}$$

with

$$K=(1-\omega)c_2+(1-\omega^2)c_3. \tag{42}$$

Here a complex number scheme has been used, with σ set equal to $(\sigma_{11}+i\sigma_\perp)$. In this expression σ_{11} is the ordinary conductivity and $\sigma_\perp$ is the Hall conductivity. The quantity ω is equal to $e^{i2\pi/3}$ and the sum rule (5) has been used to eliminate c_1. The scale factor is such that in the limit of complete breakdown $\sigma_\perp H$ is equal to $-\frac{1}{2}\pi$. The condition that σ_{11} be non-negative requires

$$c_2+c_3\geqslant c_2^2+c_3^2+c_2c_3. \tag{43}$$

In the high-field region $(H/H_B)^{1/2}\gg1$, the reflection amplitude ρ is of order $(H_B/H)^{1/2}$ and $|\tau|$ is unity plus a term of order ρ^2. The Hall term $\sigma_\perp H$ is dominated by the quantity $-\frac{1}{2}\pi$ and the corrections will not be treated further. The leading term in $\sigma_{11}H$ is of order H^{-1} or ρ^2. For simplicity we shall only consider the terms of order ρ^2 and ρ^3. Then it can be seen quite simply that we may take the magnitude of τ as unity. As a further simplification we shall set $\tau=1$ and then by unitarity ρ is pure imaginary. To this order the condition (43) is $c_2+c_3\geqslant0$.

Instead of the diagrams of Fig. 6, we shall use a set of diagrams (Fig. 9) containing up to three reflections. Moreover the triangles will be considered explicitly. Of the diagrams in Fig. 9, only (a) contributes to c_3 and the others contribute to c_2. The contributions are

$$\begin{aligned}
&\text{(a), (b):} && \rho^*\rho,\\
&\text{(c):} && 2\,\mathrm{Re}(\rho^*\rho e^{iL}),\\
&\text{(d):} && 2\,\mathrm{Re}(\rho^*\rho^2 e^{iT}),\\
&\text{(e), (f):} && 2\,\mathrm{Re}(\rho^*\rho^2 e^{i(2L-T)}),\\
&\text{(g):} && 2\,\mathrm{Re}(\rho^*\rho^2 e^{i(3L-T)}).
\end{aligned}$$

There are four more diagrams with three reflections. Two of them (h, i) are the same as Fig. 6 (h, i). The third (j) has one path going to A_3 (Fig. 1) as in Fig. 9(a), and the other path goes around one lens through A_1 and then around another lens through A_2 and terminates at A_3. These diagrams contribute to c_3. The fourth (k) has one path going around a triangle as in Fig. 9(d) and the other path going around the lens through A_1 as in Fig. 9(c). This diagram contributes to c_2. The contributions are

$$\begin{aligned}
&\text{(h), (i):} && 2\,\mathrm{Re}(\rho^*\rho^2 e^{i(L-T)}),\\
&\text{(j):} && 2\,\mathrm{Re}(\rho^*\rho^2 e^{i(2L-T)}),\\
&\text{(k):} && 2\,\mathrm{Re}(\rho^{*2}\rho e^{i(L-T)}).
\end{aligned}$$

We observe that the lens oscillations come in in second order while the triangular oscillations come in in third order. It is immediately obvious that $c_2+c_3=0$ in second order for $e^{iL}=-1$. Thus at high fields the lens orbits sweep the conductivity from zero up to twice the average value.

The triangular orbits enter in third order, by (d). We note that when $e^{iL}=-1$ this contribution can violate the rule $c_2+c_3\geqslant0$. To prevent this happening it is necessary to include the remaining diagrams. Then for $e^{iL}=-1$ the third-order contributions vanish as well since ρ is pure imaginary. But we observe that it is necessary to employ diagrams with two and three lenses to prevent the violation. In consequence the conductivity as calculated by the diagrams of Sec. 5 may come out negative at the bottom of some of the oscillations, since they include diagrams with only one lens. A similar analytic check on the fourth-order diagrams (with four reflections) would be very cumbersome, but the author verified numerically that summing

a set of diagrams including all the fourth-order ones gave oscillations which went only slightly negative and it was a marked improvement on a summation including all the third-order diagrams but not all the fourth-order diagrams. This suggests that the violations of (43) may just be a consequence of a limited summation. A similar situation occurs in evaluating the density of states by summing the diagrams for Δ, where a limited sum can give negative answers. [For instance, this can happen in (39) if $|r|^2>\frac{1}{2}$.]

Computations were also carried out for the "zone" oscillations using the diagrams of Sec. 5. It was found that the oscillations were of the same order as the average conductivity for $H\approx 3H_B$, but negative conductivities were not obtained in this case. The magnitude was strongly modulated by the triangle oscillation. The magnitude fell for H going away from $3H_B$. Not too much weight should be attached to these results because of the neglect of other diagrams with the same area. [Thus in the high-field limit the diagrams chosen give a contribution of order ρ^4 (or H^{-2}), but the diagram in Fig. 8(d), which has not been included, is of order ρ^3.] However, it seems that the oscillations should be experimentally observable. They are unique in that they are not susceptible to "thermal washout" and are not severely reduced by the integration over k_z since the area is determined by the lattice parameters only, and is independent of k_z and the energy. Thus provided a very good sample can be made so that phase coherence can be maintained, the oscillations should be extraordinarily strong.

ACKNOWLEDGMENTS

The author would like to thank Dr. R. Young for showing him Professor R. W. Stark's results for the lens-orbit oscillations prior to publication and for drawing his attention to the problem. He would also like to thank Dr. J. Essam for the reference to the basic Kubo formula.

PHYSICAL REVIEW VOLUME 165, NUMBER 3 15 JANUARY 1968

Linear Magnetoresistance in the Quantum Limit in Graphite

J. W. McClure* and W. J. Spry†
Union Carbide Corporation, Carbon Products Division, Cleveland, Ohio
(Received 21 August 1967)

Measurements of the galvanomagnetic properties of single-crystal graphite were made at 4.2°K in pulsed magnetic fields up to 160 kG. With the magnetic field parallel to the c axis, the transverse magnetoresistance is approximately proportional to the magnetic field strength, and the Hall coefficient is constant above about 80 kG. The results imply that both the diagonal and off-diagonal elements of the magnetoconductivity tensor are inversely proportional to the magnetic field strength. The results are explained theoretically using the following facts: (1) both electrons and holes occupy their lowest Landau levels for fields stronger than about 60 kG, (2) degenerate statistics apply throughout the field range, and (3) the scattering is by ionized impurities whose range depends upon the magnetic field strength. The effect provides a simple way to determine the concentration of scattering centers in graphite. It is also definitely established that the concentration of excess carriers must be determined from the off-diagonal magnetoconductivity; use of the high-field Hall coefficient alone leads to large errors.

I. INTRODUCTION

PREVIOUS investigations[1–4] of the galvanomagnetic properties of graphite single crystals have been for magnetic fields not exceeding 25 kG, though investigations of the de Haas–van Alphen oscillations in the magnetic susceptibility[5,6] have extended up to 85 kG. These investigations have provided a great deal of information about the properties of the current carriers and the energy band structure. The present work extends the measurements of galvanomagnetic properties up to field strengths of 160 kG. The measurements of the transverse magnetoresistance and Hall coefficient of a graphite single crystal with the magnetic field parallel to the c axis were carried out at 4.2°K.

Above 60 kG, graphite is in the quantum limit regime, the term being coined by Adams and Holstein[7] to indicate that all carriers in each group occupy the lowest Landau level for the group. In this region, we have found that the magnetoresistance varies linearly with

* Present address, Department of Physics, University of Oregon, Eugene, Ore.
† Present address, Carborundum Company, P.O. Box 337, Niagara Falls, N.Y.

[1] G. H. Kinchin, Proc. Roy. Soc. (London) A217, 9 (1953).
[2] T. G. Berlincourt and M. C. Steele, Phys. Rev. 98, 956 (1955).
[3] D. E. Soule, Phys. Rev. 112, 698, 708 (1958).
[4] D. E. Soule, J. W. McClure, and L. B. Smith, Phys. Rev. 134, A453 (1964),
[5] W. J. Spry and P. M. Scherer, Phys. Rev. 120, 826 (1960).
[6] S. J. Williamson, S. Foner, and M. S. Dresselhaus, Phys. Rev. 140, A1429 (1965).
[7] E. N. Adams and T. D. Holstein, J. Phys. Chem. Solids 10, 254 (1959).